

HYPERFINE STRUCTURE IN NEUTRAL MANGANESE, $Mn I$.

BY H. E. WHITE* AND R. RITSCHL

PHYSIKALISCH-TECHNISCHE REICHSANSTALT, BERLIN

(Received March 5, 1930)

ABSTRACT

Observations. The hyperfine structure patterns of some 30 or 40 lines in the spectrum of $Mn I$ have been photographed by means of a prism spectrograph and silvered Fabry-Perot etalons. A tube, designed by Schüler, and operated at liquid air temperatures, has been used as a light source for most of the lines and a king vacuum furnace for the others. Patterns of from 2 to 6 components are found, some degrading in intensity and intervals toward low frequencies and others toward higher frequencies.

Interpretation. The strictly LS coupling in the well-known multiplet structure of $Mn I$, and Ji coupling in the hyperfine structure enable vector diagrams to be drawn for the space quantization of each valence electron with respect to the nucleus. Some of the hyperfine structure terms are computed directly from observed term differences while others are computed from the observed diagonal components. The normal state ${}^6S_{5/2}(3d^54s^2)$ is found to be quite narrow, whereas the metastable ${}^6D(3d^54s)$ terms show the widest separations. While the hyperfine structure intervals for any given term are proportional to $\cos(Ji)$, the total separations are approximately determined by $\cos(Si)$, the l values of the electrons contributing but very little.

Theoretical computations. A study of the vector diagrams for the different multiplet terms shows quite definitely that while the hyperfine structure is determined primarily by the coupling between the $4s$ electron and the nucleus, the remaining valence electrons must also be taken into account. The hyperfine structure formula given by Goudsmit and Bacher for the interaction between an s electron spin and the nuclear spin is extended so as to include not only the spins of all of the valence electrons but their l values as well. From the derived general formula and the observed hyperfine structure term separations, coupling constants to be associated with each electron have been computed. While the energy of interaction between electron spin s and nuclear spin i is given by $ais \cos(is)$ the energy of interaction between electron l value and nuclear spin i is given by $ail \cos(il)$.

THE hyperfine structure in the spectral lines of neutral manganese was investigated in this laboratory by Janicki¹ some twenty years ago and later verified by Wali-Mohammed.² An analysis of the gross or multiplet structure of $Mn I$ was first given by Catalan,³ some of the terms being later assigned to definite electron configurations by Hund.⁴ A more complete analysis of the gross structure has been given by Russell⁵ and by McLennan,

* National Research Fellow.

¹ Janicki, Ann. d. Physik **29**, 833 (1909).² Wali-Mohammed, Astrophys. J. **39**, 198 (1914).³ Catalan, Phil. Trans. Roy. Soc. London **223**, 127 (1923).⁴ Hund, Linienspektren, p. 161, 1927.⁵ Russell, Astrophys. J. **66**, 184 (1927).

McLay and Crawford.⁶ Since the *hfs*⁷ of many of the lines is observed to have the same general appearance as that found in a number of other elements (for example, praseodymium, lanthanum, iodine, and bromine) it was hoped that an analysis of the *hfs*, at the expense of the well-known *gs*, would not only verify the interpretation of *hfs* given previously by one of the authors,⁸ but at the same time to lead to some conclusions concerning *hfs* in general.

APPARATUS AND MEASUREMENTS

A Zeiss three-prism constant deviation spectrograph, with a large glass optical system specially constructed for fine-structure work, was used in conjunction with quartz Fabry-Perot etalons for photographing the *hfs*. In order to eliminate self-reversal of resonance lines and at the same time to

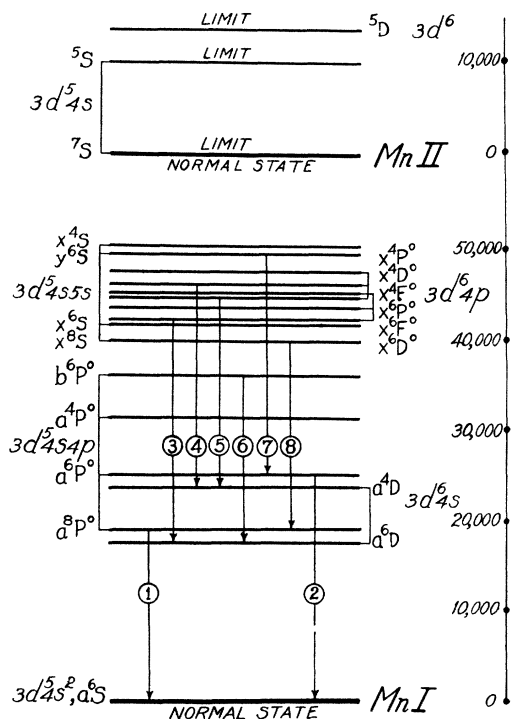


Fig. 1. Term scheme of neutral manganese, Mn I.

produce very sharp lines, a metal discharge tube, operated at liquid air temperatures, has been used. Prior to publication, the design and operation of this tube was very kindly submitted to the authors by Dr. Schüler.⁹ The manganese lines were excited in a discharge of argon by placing small pieces

⁶ McLennan, McLay and Crawford, *Trans. Roy. Soc. Canada* **20**, 15 (1926).

⁷ The words hyperfine structure and gross structure will be abbreviated by *hfs* and *gs* respectively.

⁸ White, *Phys. Rev.* **34**, 1404 (1929); *Proc. Nat. Acad. Sci.* **16**, 68 (1930).

⁹ Schüler, *Zeits. f. Physik* **59**, 149 (1930).

TABLE I. Measured *hfs*-components in Mn I.

Mult. No.	Design.	λ ν	$\Delta\lambda_1$ $\Delta\nu_1$	$\Delta\lambda_2$ $\Delta\nu_2$	$\Delta\lambda_3$ $\Delta\nu_3$	$\Delta\lambda_4$ $\Delta\nu_4$	$\Delta\lambda_6$ $\Delta\nu_6$	Total $\Delta\lambda$ Total $\Delta\nu$
1	${}^6S_{21} - {}^8P_{31}^0$ ${}^6S_{21} - {}^8P_{21}^0$	5394.677	+ .0325	+ .0285	+ .0230	+ .0200	+ .0111	+ .1151
		18531.65	- .1116	- .0979	- .0790	- .0687	- .0381	- .3953
		5432.555 18402.45	+ .0306 - .1036	+ .0247 - .0836	+ .0198 - .0671	+ .0133 - .0450	+ .0884 - .2993	
2	${}^6S_{21} - {}^6P_{31}^0$ ${}^6S_{21} - {}^6P_{21}^0$ ${}^6S_{21} - {}^6P_{11}^0$	4030.760	+ .0155	+ .0133	+ .0104	+ .0079	+ .0052	+ .0523
		24802.23	- .0930	- .0798	- .0624	- .0474	- .0312	- .3138
		4033.074 24788.01 4034.489 24779.31	+ .0142 - .0873 + .0145 - .0891	+ .0127 - .0781 + .0117 - .0719	+ .0090 - .0553 + .0077 - .0473	+ .0060 - .0369	+ .0419 - .2576 + .0339 - .2083	
3	${}^6D_{41} - {}^6D_{31}^0$ ${}^6D_{31} - {}^6D_{21}^0$ ${}^6D_{41} - {}^6D_{41}^0$ ${}^6D_{21} - {}^6D_{11}^0$ ${}^6D_{31} - {}^6D_{31}^0$ ${}^6D_{21} - {}^6D_{21}^0$ ${}^6D_{31} - {}^6D_{41}^0$ ${}^6D_{11} - {}^6D_{11}^0$ ${}^6D_{11} - {}^6D_{21}^0$ ${}^6D_{21} - {}^6D_{31}^0$	4018.108	- .0192	- .0155	- .0129	- .0100		- .0651
		24880.32	+ .1188	+ .0959	+ .0799	+ .0619		+ .4029
		4035.730	- .0159	- .0135	- .0107			- .0507
		24771.69	+ .0976	+ .0829	+ .0657			+ .3113
		4041.366	- .0165	- .0140	- .0116	- .0093	- .0060	- .0574
		24737.15	+ .1010	+ .0857	+ .0710	+ .0569	+ .0367	+ .3513
		4048.760	- .0146	- .0125	- .0098			- .0369
		24691.97	+ .0890	+ .0763	+ .0598			+ .2251
		4055.553	- .0142	- .0122	- .0099	- .0070		- .0481
		24650.62	+ .0863	+ .0742	+ .0602	+ .0426		+ .2925
		4063.533	- .0133	- .0102				- .0364
		24602.18	+ .0807	+ .0619				+ .2209
		4079.245	- .0139	- .0110	- .0082			- .0436
		24507.44	+ .0834	+ .0660	+ .0492			+ .2616
		4079.428	- .0197					- .0197
24506.34	+ .1182					+ .1182		
4082.947	- .0112	- .0091	- .0070			- .0273		
24485.22	+ .0672	+ .0546	+ .0420			+ .1638		
4083.639	- .0109					- .0326		
24481.07	+ .0654					+ .1956		

TABLE I (continued).

4	${}^4D_{1\frac{1}{2}} - {}^4D_{\frac{3}{2}}^0$	4453.013 22450.42	+ .0172 - .0867			+ .0172 - .0867	
	${}^4D_{\frac{1}{2}} - {}^4D_{\frac{3}{2}}^0$	4472.793 22351.14	- .0229 + .1145	- .0162 + .0810		- .0391 + .1955	
	${}^4D_{\frac{3}{2}} - {}^4D_{1\frac{1}{2}}^0$	4490.078 22265.10	- .0235 + .1165			- .0235 + .1165	
5	${}^4D_{3\frac{1}{2}} - {}^4F_{3\frac{1}{2}}^0$	4709.704 21226.83	+ .0133 - .0599			+ .0420 - .1893	
	${}^4D_{2\frac{1}{2}} - {}^4F_{2\frac{1}{2}}^0$	4727.462 21147.10	+ .0152 - .0697			+ .0421 - .1883	
6	${}^6D_{4\frac{1}{2}} - {}^6P_{3\frac{1}{2}}^0$	5341.070 18717.64	- .0628 + .2201	- .0530 + .1857	- .0438 + .1535	- .2170 + .7605	
	${}^6D_{3\frac{1}{2}} - {}^6P_{3\frac{1}{2}}^0$	5407.432 18487.97	- .0552 + .1888	- .0445 + .1522		- .1627 + .5564	
	${}^6D_{3\frac{1}{2}} - {}^6P_{2\frac{1}{2}}^0$	5420.368 18443.82	- .0581 + .1976	- .0467 + .1589	- .0348 + .1184	- .1846 + .6279	
	${}^6D_{2\frac{1}{2}} - {}^6P_{3\frac{1}{2}}^0$	5457.468 18318.44	- .0508 + .1705	- .0408 + .1369		- .1423 + .4777	
	${}^6D_{2\frac{1}{2}} - {}^6P_{2\frac{1}{2}}^0$	5470.640 18274.33	- .0545 + .1821	- .0435 + .1453		- .1484 + .4958	
	${}^6D_{2\frac{1}{2}} - {}^6P_{1\frac{1}{2}}^0$	5481.395 18238.48	- .0662 + .2203	- .0512 + .1704	- .0365 + .1215	- .1539 + .5122	
	${}^6D_{1\frac{1}{2}} - {}^6P_{2\frac{1}{2}}^0$	5505.877 18157.38	- .0484 + .1597	- .0413 + .1362		- .1189 + .3922	
	${}^6D_{1\frac{1}{2}} - {}^6P_{1\frac{1}{2}}^0$	5516.773 18121.52	- .0748 + .2458	- .0498 + .1636		- .1246 + .4094	
	${}^6D_{\frac{1}{2}} - {}^6P_{1\frac{1}{2}}^0$	5537.749 18052.88	- .1116 + .3640			- .1116 + .3640	
	7	${}^6P_{3\frac{1}{2}} - {}^6S_{2\frac{1}{2}}^0$	4061.744 24613.03	- .0326 + .1975	- .0290 + .1757	- .0210? + .1272?	- .1066? + .6458?

of manganese metal in the tube, the discharge itself taking place in a small cylinder, 2 cm long and 1 cm in diameter, working as a Paschen hollow cathode, in the bottom of the tube. The light from the discharge was reflected into a horizontal position by a plane mirror and then brought to focus on the slit of the spectrograph. With a current of 100 to 200 m.a. at about 2500 volts d.c., exposure times at 4000A ranged from 1 to 5 minutes. In the absence of hydrogen, and at the right pressure, the manganese lines were stronger than those of argon. With silvered quartz mirrors, separated by invar rings 5, 7.5, 10, 12, and 15 mm in thickness, placed between the collimating lens and the prisms, a resolving power of nearly one million at 4000A has been obtained. The mirrors were silvered in vacuum by evaporation from electrically heated silver filaments, a method developed previously by one of the authors.¹⁰ While the lines photographed have the same appearance as those found in praseodymium,¹¹ they are in general about one-fifth to one tenth as wide and vary in number from one to six components.

An energy level diagram of Mn I is given in Fig. 1. Each *gs*-multiplet, for which the *hfs* has been studied, is shown by a transition arrow and assigned a number for reference in Tables I and II. All of the lines except those in multiplets numbered six and seven, have been photographed with the light source at liquid air temperatures, thus enabling the *hfs* $\Delta\lambda$'s in Tables I and II to be given to four decimal places. The last two multiplets, numbers six and

TABLE II. Measured *hfs*-components in Mn I.

Mult. No.	Design	λ ν	Total $\Delta\lambda$ Total $\Delta\nu$	Mult. No.	Design	λ ν	Total $\Delta\lambda$ Total $\Delta\nu$
4	$^4D_{3\frac{1}{2}} - ^4D_{2\frac{1}{2}}^0$	4414.887 22644.29	+ .0264? - .1352?	4	$^4D_{1\frac{1}{2}} - ^4D_{2\frac{1}{2}}^0$	4498.897 22221.45	sharp
	$^4D_{2\frac{1}{2}} - ^4D_{1\frac{1}{2}}^0$	4436.358 22534.70	+ .0226 - .1148		$^4D_{2\frac{1}{2}} - ^4D_{3\frac{1}{2}}^0$	4502.223 22205.01	+ .0244 - .1204
	$^4D_{3\frac{1}{2}} - ^4D_{3\frac{3}{2}}^0$	4451.578 22457.66	+ .0274 - .1383	7	$^6P_{1\frac{1}{2}}^0 - ^6S_{2\frac{1}{2}}$	4057.959 24635.99	- .0792 + .4810
	$^4D_{2\frac{1}{2}} - ^4D_{2\frac{3}{2}}^0$	4464.679 22391.76	+ .0236 - .1184		$^6P_{2\frac{1}{2}}^0 - ^6S_{2\frac{1}{2}}$	4059.399 24627.26	- .0850 + .5160
	$^4D_{1\frac{1}{2}} - ^4D_{1\frac{3}{2}}^0$	4470.142 22364.40	sharp				

seven, were photographed using as a light source a King vacuum furnace operated at about 2000°C. Fortunately these two multiplets show the widest *hfs* in Mn I, thus making it possible to resolve some of the patterns at this temperature. The manganese lines were brought out much stronger than is usually obtained from such a furnace by applying a potential of 120 volts d.c. between a small anode and the heating element of the furnace.¹² The anode is

¹⁰ Ritschl, Verhand. d. Deutsch. Phys. Ges. (3), 10, 33 (1929).

¹¹ White, Phys. Rev. 34, 1397 (1929).

¹² Schüler, Zeits. f. Physik 37, 728 (1926).

here placed coaxial with and extends half way through the heated graphite tube of the furnace.¹⁰ Since the relative intensities of the components in each pattern are always found to decrease regularly toward longer or shorter wave-lengths, the wave-length and frequency number of only the strongest component in each pattern is given in column three. The wave-lengths and frequency numbers of the other components may be obtained by adding or subtracting, as the case may be, the $\Delta\lambda$'s and $\Delta\nu$'s given in columns four, five, six, seven and eight. Where only the first two, three, or four components of a group are resolved, the end of the group has been measured. The total

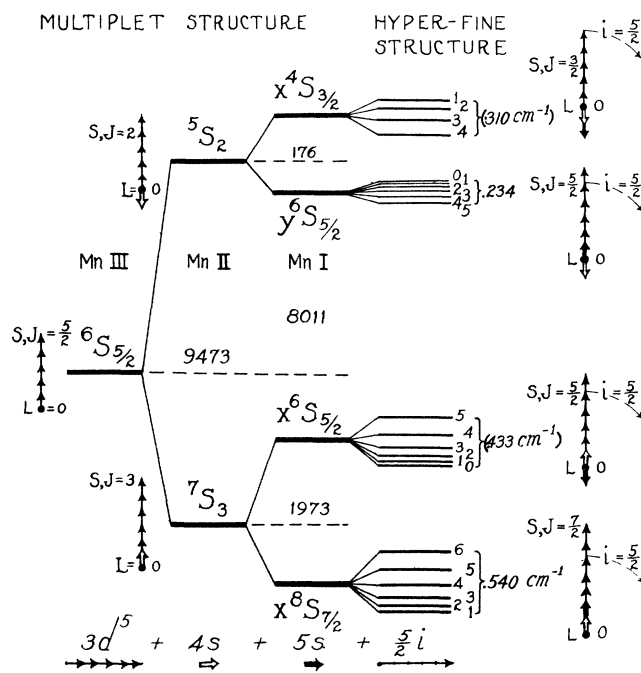


Fig. 2. Hyperfine structure terms and space quantization vectors for the electron configuration $3d^5 4s 5s$.

width of each pattern is given in the last column. In general the measurements given by Janicki¹ are in good agreement with those in Tables I and II. The additional component which Janicki found on the short wave-length side of $\lambda\lambda 4030, 4033$ and 4034 is very probably a self-reversal effect of each *hfs*-component, and, is not found on any of our plates. At liquid air temperatures very sharp and well-resolved patterns of these three lines have been photographed. As reported by Janicki, $\lambda\lambda 6021, 6016,$ and 6013 appear sharp. Although these lines are quite strongly excited at liquid air temperatures and are visually seen to be quite narrow, they have not been photographed due to the extremely long exposures necessary at this wave-length.

Owing to an early mistake in the width of an etalon ring, the computations reported in a brief note, "Letters to the Editor" in the Physical Review,¹³ are

¹³ White and Ritschl, Phys. Rev. 35, 208 (1930).

in error. The $\Delta\lambda$'s and $\Delta\nu$'s for the two lines there given may be corrected by multiplying by a factor of 1.25.

THE COMPUTATION AND INTERPRETATION OF THE *HFS*-TERM SEPARATIONS

There are two distinct and characteristic systems of multiplet terms in the arc spectrum of manganese, as may be seen from Fig. 1; (a) a system of *normal* multiplet terms built upon the 5S and 7S ($3d^54s$) terms of Mn II, which in turn are built upon the 6S ($3d^5$) term of Mn III, and (b) a system of inverted multiplet terms built upon the inverted 5D ($3d^6$) term of Mn II. It has been indicated previously⁸ that the *hfs* of manganese is in good agreement with the

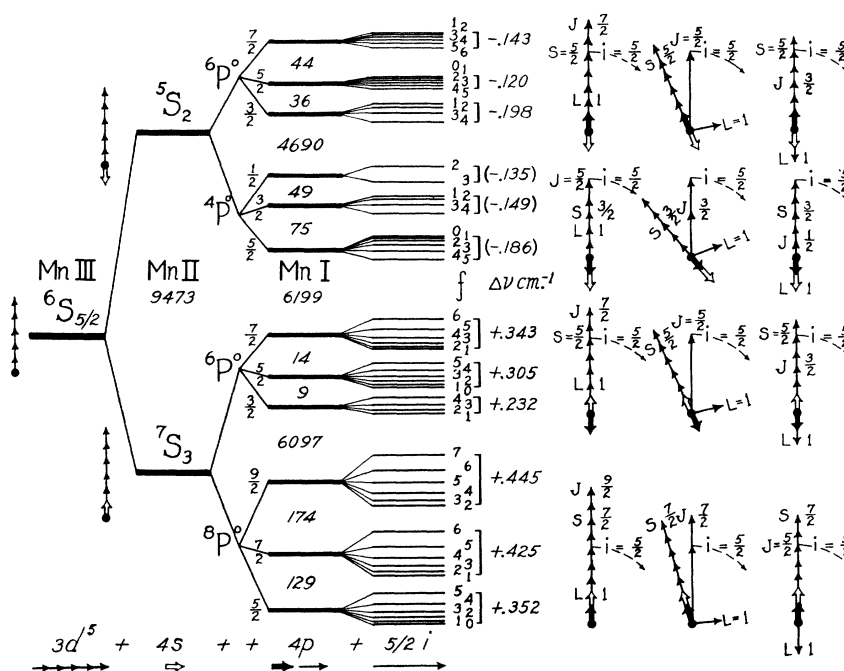


Fig. 3. Multiplet structure terms, *hfs*-terms, and space quantization vectors for the electron configuration $3d^5 4s^2 4p^1 5/2 i$.

interpretation of *hfs* in other elements. Here in manganese, as in many other elements, the deep penetrating and tightly bound *s* electron is found to play an important role. The coupling of a $4s$ electron with the resultant of six other valence electrons is observed to give the widest *gs*-separations while its strong coupling with the nucleus gives rise to the widest *hfs*-separations. Fortunately, *LS* coupling in the *gs* and *Ji* coupling in the *hfs* is quite rigidly held to, thus enabling vector diagrams for the space quantization of the *s* and *l* values for each valence electron to be quite accurately drawn. It has also been previously shown⁸ that the total *hfs*-separation of a *gs*-term should be approximately proportional to $\cos(is)$, where *s* is the spin of the deeply penetrating and tightly bound *s* electron, and *i* is the nuclear spin momentum. Since this proportionality is taken for the vector position $\cos(Ji) = 1$, where

$\cos(is) = \cos(Js)$, it may be stated that for each gs -term where $\cos(Js)$ is *positive*, the hfs -terms are *normal*, and where $\cos(Js)$ is *negative* the hfs -terms are *inverted*.

At the left in Fig. 2 the building up of the x^4S , x^6S , y^6S , and x^8S ($3d^54s5s$) terms of Mn I is shown starting with the parent term 6S ($3d^5$) of Mn III. This is done in order to show the direction taken on by the spins of the 4s and 5s electrons in each gs -term and to show the shift in energy due to the inversion (with respect to the electron resultant J) of either the 4s or 5s electron. At the right in Fig. 2, it may be seen that when the 4s electron spin is parallel with J , $\cos(Js_{4s})$ positive, the hfs -terms are *normal*, and when oppositely directed, $\cos(Js_{4s})$ negative, the hfs -terms are *inverted*. Space quantization of i with J and s is only shown for the position of largest f value.

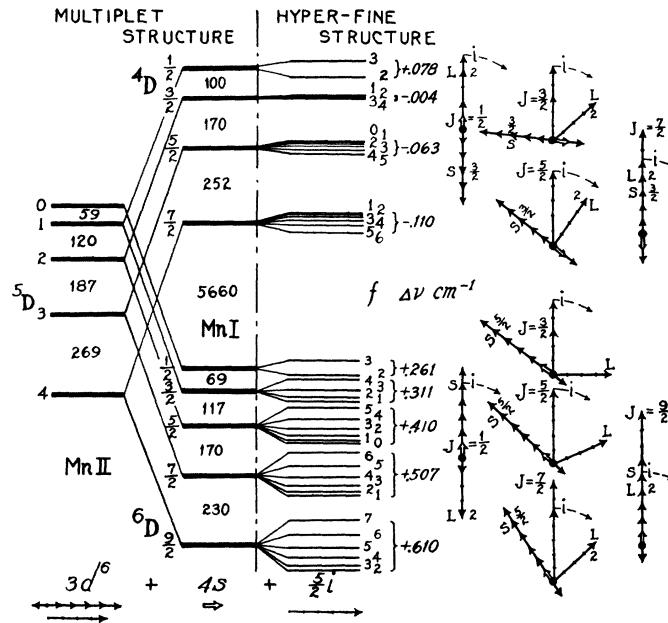


Fig. 4. Hyperfine structure terms and space quantization vectors for the electron configuration $3d^54s$.

The building up of the a^4P^0 , a^6P^0 , b^6P^0 , and a^8P^0 ($3d^54s4p$) terms in Fig. 3 is quite similar to that of the x^4S , x^6S , y^6S and x^8S terms in Fig. 2. The addition of a $4p$ electron, with quantum number $s = \frac{1}{2}$ and $l = 1$, in place of a $5s$ electron, with $s = \frac{1}{2}$ and $l = 0$, however, splits both 5S and 7S ($3d^54s$) of Mn II into six levels in place of two. The vector diagrams for each level are given at the right in Fig. 3. For each gs -level of a^4P^0 and b^6P^0 , $\cos(Js_{4s})$ negative, the hfs -terms are *inverted*, whereas, for a^6P^0 and a^8P^0 , $\cos(Js_{4s})$ positive, the hfs -terms are *normal*.

Starting with the inverted 5D ($3d^5$) term of Mn II at the left in Fig. 4, the addition of a $4s$ electron splits each level into two levels resulting in the *inverted* multiplet terms a^4D and a^6D ($3d^54s$). Here again for $\cos(Js_{4s})$ negative, the hfs -terms are *inverted*, while for $\cos(Js_{4s})$ positive they are *normal*.

The stepwise inversion of the *hfs* in the four terms of a^4D follows directly from the stepwise change from positive $\cos(Js_{4s})$ in $a^4D_{3/2}$ to negative $\cos(Js_{4s})$ in $a^4D_{5/2}$.

Each spectral line in manganese is in reality a tiny multiplet. Several characteristic types of these *hfs*-multiplets are shown in Figs. 5 and 6. A new Zeiss microphotometer, having variable magnification, has been used to obtain density curves from the best plates, copies of which are shown at the bottom of the figures. From the total width of lines of the type shown in Fig. 5, it is obvious why only the *diagonal* lines have been resolved and measured. The intervals between the *diagonal* lines give only the difference between the

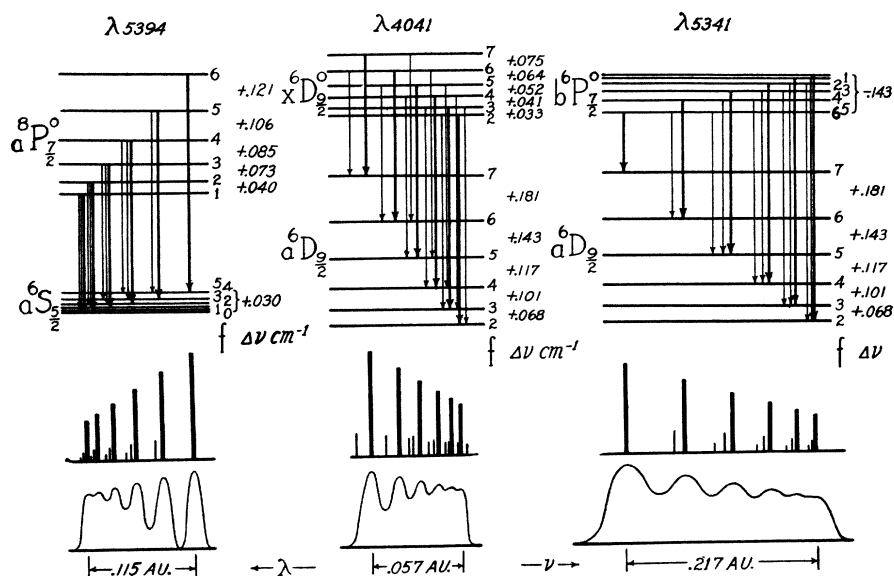


Fig. 5. Hyperfine structure patterns in neutral manganese. $\lambda\lambda 5394$ and 4041 taken at liquid air temperatures and $\lambda 5341$ taken from a vacuum furnace.

set of levels above and the set below. It should here be pointed out that the total width of $\lambda 4041$ is only 0.057\AA . It was hoped, therefore, in a wide pattern of lines like $\lambda 5341$, Fig. 5, that the *off diagonal*, or faint lines, could be observed. Since the *gs*-multiplet to which this line belongs was so weakly excited in the Schüller tube, and at the same time lies in a region of the spectrum where photographic plates are rather insensitive, the vacuum furnace was resorted to. The only trace of the *off diagonal*, or faint lines, in any of the *hfs*-multiplets has been found in the lines $a^8P^0_{4\frac{1}{2}, 3\frac{1}{2}, 2\frac{1}{2}}, -x^8S_{3\frac{1}{2}}$. All three lines of this *gs*-multiplet, $\lambda\lambda 4823, 4783, \text{ and } 4754$, are shown in Fig. 6. Even though the extremely narrow patterns of these lines have not been completely resolved, their interpretation is quite unambiguous since their general appearance verifies the order and magnitude of the *hfs*-term separations of a^8P^0 and x^8S arrived at from other considerations. What has actually been measured is indicated at the bottom of the figure. The five *off diagonal* lines on the low frequency side of $\lambda 4783$ fortunately fall almost together and can be

measured as a single strong component. With the measured separations between this component and the first two diagonal components and, making the valid assumption that the Landé interval rule is in operation, the x^8S , and in turn the a^8P^0 , hfs -term separations can be approximately computed. With this as a start, the total separation of the normal state ${}^6S_{7/2}$ ($3d^54s^2$) is determined from the two resonance lines $\lambda\lambda 5394$ and 5432 to be about 0.030 cm^{-1} . The separations for $a^6P^0_{3/2, 2/2, 1/2}$ are then determined from $\lambda\lambda 4030, 4033,$ and 4034 . While the hfs -patterns of ${}^6D-{}^6D^0$ and ${}^4D-{}^4D^0$ ($3d^64s-3d^64p$)

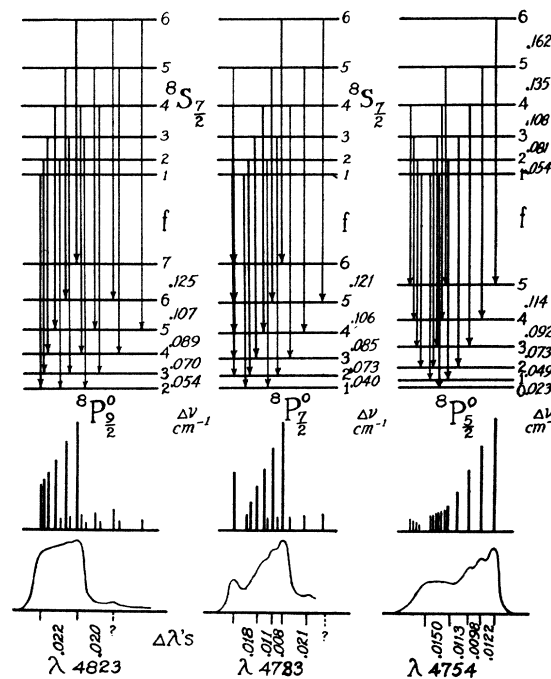


Fig. 6. Very narrow hyperfine structure patterns in the octet system of manganese taken at liquid air temperatures.

have been obtained at liquid air temperatures, none of them resolve the *off diagonal* components that must certainly be there. From the measured differences between the different patterns of a multiplet, however, a clue to the hfs -separations is obtained. The successive differences, for example, between the $\Delta\nu$'s of $\lambda\lambda 4018, 4055$ and 4083 as compared with the successive differences between the $\Delta\nu$'s of $\lambda\lambda 4079, 4055$ and 4035 show that the a^6D ($3d^64s$) separations are about two and one-half times as wide as those of x^6D^0 ($3d^64p$). Even though relations of this kind can only give, at best, an approximation to the true separations, it has been necessary to use such relations to compute the separations for $a^6D, b^6P^0, a^4D, x^6D^0$ and x^4D^0 . The gs -terms and hfs -term intervals are given in Table III.

THEORETICAL INTERPRETATION

It has quite generally been observed that the widest hfs -separations are due to the strong coupling between the spin of a single s electron and the nu-

TABLE III. *hfs-term intervals, Mn I.*

Term	Value	$\Delta\nu_1$	$\Delta\nu_2$	$\Delta\nu_3$	$\Delta\nu_4$	$\Delta\nu_5$	Total $\Delta\nu$
$a^6S_{2\frac{1}{2}}$	59937.47	+ .010	+ .008	+ .006	+ .004	+ .002	+ .030
$x^8S_{3\frac{1}{2}}$	20506.13	+ .162	+ .135	+ .108	+ .081	+ .054	+ .540
$x^6S_{2\frac{1}{2}}$	18533.50	+ .144	+ .115	+ .087	+ .058	+ .029	+ .433
$\gamma^6S_{2\frac{1}{2}}$	10524.27	- .078	- .062	- .047	- .031	- .016	- .234
$x^4S_{1\frac{1}{2}}$	10346.03	- .138	- .103	- .069			- .310
$a^8P_{4\frac{1}{2}}^0$	41232.09	+ .125	+ .107	+ .089	+ .070	+ .054	+ .445
$a^8P_{3\frac{1}{2}}^0$	41405.80	+ .121	+ .106	+ .085	+ .073	+ .040	+ .425
$a^8P_{2\frac{1}{2}}^0$	41534.98	+ .114	+ .092	+ .073	+ .049	+ .023	+ .352
$a^6P_{3\frac{1}{2}}^0$	35135.24	+ .103	+ .088	+ .068	+ .051	+ .033	+ .343
$a^6P_{2\frac{1}{2}}^0$	35149.46	+ .097	+ .086	+ .061	+ .041	+ .020	+ .305
$a^6P_{1\frac{1}{2}}^0$	35158.16	+ .099	+ .080	+ .053			+ .232
$b^6P_{3\frac{1}{2}}^0$	24167.53	- .044	- .037	- .030	- .019	- .013	- .143
$b^6P_{2\frac{1}{2}}^0$	24211.65	- .040	- .032	- .022	- .008		- .120
$b^6P_{1\frac{1}{2}}^0$	24247.40	- .100	- .060	- .038			- .198
$a^4P_{2\frac{1}{2}}^0$	28936.41	- .062	- .050	- .037	- .025	- .012	- .186
$a^4P_{1\frac{1}{2}}^0$	28861.11	- .066	- .050	- .033			- .149
$a^4P_{\frac{1}{2}}^0$	28812.58	- .135					- .135
$a^6D_{4\frac{1}{2}}$	42885.17	+ .181	+ .143	+ .117	+ .101	+ .068	+ .610
$a^6D_{3\frac{1}{2}}$	42655.50	+ .160	+ .123	+ .103	+ .073	+ .048	+ .507
$a^6D_{2\frac{1}{2}}$	42485.96	+ .142	+ .111	+ .083	+ .053	+ .021	+ .410
$a^6D_{1\frac{1}{2}}$	42368.98	+ .128	+ .104	+ .079			+ .311
$a^6D_{\frac{1}{2}}$	42300.28	+ .261					+ .261
$a^4D_{3\frac{1}{2}}$	36640.81	- .033	- .028	- .022	- .016	- .011	- .110
$a^4D_{2\frac{1}{2}}$	36388.29	- .021	- .017	- .013	- .008	- .004	- .063
$a^4D_{1\frac{1}{2}}$	36217.00	- .002	- .001	- .001			- .004
$a^4D_{\frac{1}{2}}$	36118.69	+ .078					+ .078
$x^6D_{4\frac{1}{2}}^0$	18148.04	+ .075	+ .064	+ .052	+ .041	+ .033	+ .265
$x^6D_{3\frac{1}{2}}^0$	18004.88	+ .065	+ .052	+ .042	+ .034	+ .022	+ .216
$x^6D_{2\frac{1}{2}}^0$	17883.78	+ .062	+ .050	+ .037	+ .025	+ .012	+ .186
$x^6D_{1\frac{1}{2}}^0$	17793.97	+ .057	+ .043	+ .028			+ .128
$x^6D_{\frac{1}{2}}^0$	17738.89	+ .092					+ .092

clear spin i , and also that the observed intervals follow the Landé interval rule. Since the classical quantum mechanics have yielded interval rules which agree so well with observations in gs -multiplets, Goudsmit and Bacher¹⁴ have extended them to some of the simpler cases in hfs . The Landé interval rule for separations between two states f and $(f+1)$ is, as in gs , given by $\Delta\nu = A(f+1)$, where f is the resultant of i and J , and A is an observed proportionality constant. The total separation of a multiplet term is given by

$$\Delta\nu = mA \quad (1)$$

where $m = \sum f$'s minus the smallest f .

Assuming the cosine law for the interaction energy of any two electronic angular momentum vectors, the energy of interaction between an s electron spin and the nuclear spin, i , as shown by Goudsmit and Bacher and others, may be written

$$ais \cos(is). \quad (2)$$

Since i and s are constants, a is a constant to be associated with the electron, its value depending upon how strongly the electron spin is coupled with the nucleus spin.

¹⁴ Goudsmit and Bacher, Phys. Rev. **34**, 1501 (1929).

In the case of an s electron and an arbitrary other electron, in LS coupling,

$$a_1 i s \overline{\cos(is_1)} = a_1 i s_1 \cos(ij) \cos(js) \cos(ss_1) = A ij \cos(ij) \quad (3)$$

where in terms of the quantum mechanics cosines

$$A = a_1 \frac{s(s+1) + s_1(s_1+1) - s_2(s_2+1)}{2s(s+1)} \cdot \frac{j(j+1) + s(s+1) - l_2(l_2+1)}{2j(j+1)} \quad (4)$$

and is the A of Eq. (1). The subscripts denote the s and arbitrary electron respectively. As pointed out by Goudsmit and Bacher, this expression for A , which is also applicable in the case where an s electron is added to a more general electron configuration, takes into account only the interaction between the s electron and the nucleus and neglects the interaction of the other valence electrons. A study of the vector diagrams and hfs shown in Figs. 2, 3, and 4 shows quite definitely that while the total hfs -separations depend primarily upon the $4s$ electron, the remaining valence electrons also make some contribution, and in some cases almost equal the contribution of the $4s$ electron. We may extend Eq. (4) in such a way that it is applicable to p , d , and f electrons as well as to s electrons. This is done by assuming that the electron has only a spin s and that its l vector is associated with the remaining valence electrons. This total *remainder* is then thought of as a parent term R_1 to which an electron spin S_1 alone is added to give the resultant multiplet term under consideration. Eq. (4) is then written

$$A = a_1 \frac{S(S+1) + S_1(S_1+1) - S_{R_1}(S_{R_1}+1)}{2S(S+1)} \cdot \frac{J(J+1) + S(S+1) - L_{R_1}(L_{R_1}+1)}{2J(J+1)} \quad (5)$$

Here S_1 may represent the spin of one or more electrons and a_1 the coupling constant associated with S_1 . Making the valid assumption that the energy of interaction between an l vector and the nuclear spin i is given by

$$a i l \cos(il) \quad (6)$$

the l vectors of each valence electron may be taken into account by replacing each S and L of Eq. (5) by L and S respectively. Taking into account all of the electrons we get the general expression

$$A = \sum_n a_n \frac{S(S+1) + S_n(S_n+1) - S_{R_n}(S_{R_n}+1)}{2S(S+1)} \cdot \frac{J(J+1) + S(S+1) - L_{R_n}(L_{R_n}+1)}{2J(J+1)} + \sum_n a_n \frac{L(L+1) + L_n(L_n+1) - L_{R_n}(L_{R_n}+1)}{2L(L+1)} \cdot \frac{J(J+1) + L(L+1) - S_{R_n}(S_{R_n}+1)}{2J(J+1)} \quad (7)$$

For n valence electrons this gives A in terms of $2n$ constants. With seven valence electrons in manganese the fourteen constants are readily reduced to

TABLE IV. *hfs-coupling constants. Electron configurations 3d⁴s4p and 3d⁴s².*

Term	Total $\Delta\nu$	$R_1 R_2 R_3 R_4$	m_A	A	a_1 4s	a_2 4p	a_3 4p	a_4 3d _s
$a^3P_{4^0}$	+ .445	$7P^7P^8S^3P$	25A	$+a_3 2/9$.120	.019	.006	.002
$a^3P_{3^0}$	+ .425	$7P^7P^8S^3P$	20A	$+a_3 4/63$.124	.021	.006	.002
$a^3P_{2^0}$	+ .352	$7P^7P^8S^3P$	15A	$-a_3 2/7$.110	.018	.006	.002
$a^6P_{3^0}$	+ .343	$5P^7P^6S^1P$	20A	$+a_3 2/7$.112	.020	.006	.002
$a^6P_{2^0}$	+ .305	$5P^7P^6S^1P$	15A	$+a_3 4/35$.113	.018	.006	.002
$a^6P_{1^0}$	+ .232	$5P^7P^6S^1P$	9A	$-a_3 2/5$.105	.020	.006	.002
$b^6P_{3^0}$	- .143	$7P^6P^6S^1P$	20A	$+a_3 2/7$.125	.018	.006	.002
$b^6P_{2^0}$	- .120	$7P^6P^6S^1P$	15A	$+a_3 4/35$.112	.021	.006	.002
$b^6P_{1^0}$	- .198	$7P^6P^6S^1P$	9A	$-a_3 2/5$.137	.018	.006	.002
$a^4P_{2^0}$	- .186	$5P^5P^4S^3P$	15A	$+a_3 2/5$.118	.019	.006	.002
$a^4P_{1^0}$	- .149	$5P^5P^4S^3P$	9A	$+a_3 4/15$.118	.019	.006	.002
$a^4P_{\frac{1}{2}^0}$	- .135	$5P^5P^4S^3P$	3A	$-a_3 2/3$.118	.019	.006	.002
$a^8S_{2^0}$	+ .030	$1S_d$	15A	$+a_4$.002

TABLE V. *hfs-coupling constants. Electron configuration 3d⁶4s5s.*

Term	Total $\Delta\nu$	$R_1 R_2 R_3$	mA	A	a_1 4s _s	a_2 5s _s	a_3 3d ⁶ _s
$^3S^3S^3$	+ .540	$^7S^7S^3S$	20A	+ a_1 1/7	.149	.030	.002
$^3S^3S^3$	+ .433	$^5S^7S^1S$	15A	+ a_1 1/5	.156	.030	.002
$^3S^3S^3$	- .234	$^7S^5S^1S$	15A	- a_1 1/7	.165	.030	.002
$^3S^3S^3$	- .310	$^5S^5S^3S$	9A	- a_1 1/5	.156	.030	.002

TABLE VI. *hfs-coupling constants. Electron configuration 3d⁶4s.*

Term	Total $\Delta\nu$	$R_1 R_2 R_3$	mA	A	a_1 4s _s	a_2 3d ⁶ _s	a_3 3d ⁶ _t
$^3D^3D^3$	+ .610	$^5D^2D^6S$	25A	+ a_1 1/9	.159	.011	.004
$^3D^3D^3$	+ .507	$^5D^2D^6S$	20A	+ a_1 37/315	.158	.011	.004
$^3D^3D^3$	+ .410	$^5D^2D^6S$	15A	+ a_1 23/175	.153	.011	.004
$^3D^3D^3$	+ .311	$^5D^2D^6S$	9A	+ a_1 13/75	.153	.011	.004
$^3D^3D^3$	+ .261	$^5D^2D^6S$	3A	+ a_1 7/15	.154	.011	.004
$^3D^3D^3$	- .110	$^5D^2D^4S$	20A	- a_1 3/35	.156	.011	.004
$^3D^3D^3$	- .063	$^5D^2D^4S$	15A	- a_1 13/175	.156	.011	.004
$^3D^3D^3$	- .004	$^5D^2D^4S$	9A	- a_1 1/25	.156	.011	.004
$^3D^3D^3$	+ .078	$^5D^2D^4S$	3A	+ a_1 1/5	.156	.011	.004

three or four since five $3d$ electrons may be treated as a unit. The electron configuration $3d^5 4s 4p$, for the terms shown in Fig. 3, will here be used as an example. For the $4s$ electron with l value 0, only one constant, a_1 of Table IV, is to be determined. The contribution of a $4p$ electron with s value $\frac{1}{2}$ and l value 1 is represented by two constants, a_2 and a_3 respectively. The five $3d$ electrons, considered as a unit, have a spin value $2\frac{1}{2}$ and an l value 0 and may therefore be treated as a single s electron with spin $2\frac{1}{2}$ and represented by one constant, a_4 , Table IV.

The values of the a 's in the last four columns of Table IV may be computed from the $\Delta\nu$'s of Table III in the following manner. From Eqs. (1) and (7) and the total $\Delta\nu$'s we get for

$${}^6S_{2\frac{1}{2}}, + 0.030 = 15(\quad \quad \quad + a_4 \quad) \quad (8)$$

$${}^8P_{4\frac{1}{2}}^0, + 0.445 = 25(a_1 1/9 + a_2 1/9 + a_3 2/9 + a_4 5/9) \quad (9)$$

$${}^8P_{2\frac{1}{2}}^0, + 0.352 = 15(a_1 9/49 + a_2 9/49 - a_3 2/7 + a_4 45/49) \quad (10)$$

$${}^6P_{3\frac{1}{2}}^0, + 0.343 = 20(a_1 1/7 - a_2 5/49 + a_3 2/7 + a_4 5/7). \quad (11)$$

From the four simultaneous equations the four constants a_1 , a_2 , a_3 , and a_4 can be determined. Since a_3 and a_4 are small as compared with a_1 and a_2 they are assumed the same for all of the terms in Table IV and are set in italics. The constant a_3 for ${}^8P_{4\frac{1}{2}}^0$ for example, is the mean of six values, taking each time Eq. (9) and one of the six equations from the ${}^6P^0$ terms. The a_1 's for the $4s$ electron are then computed independently for each term, so that the four constants following each term give the total $\Delta\nu$ in column two. Since the $\Delta\nu$'s for the ${}^4P^0$ terms have not been observed they have been computed from the mean values of the a 's of the other nine P^0 terms. A method similar to that used for the P^0 terms has been used to determine the a 's for the D and S terms of the electron configurations $3d^5 4s 5s$ and $3d^6 4s$ respectively. The results are shown in Tables V and VI.

It is to be expected that the value of a_1 for the $4s$ electron obtained from each term of each electron configuration would be nearly the same. It is likewise to be expected that a_4 of Table IV and a_3 of Table VI would have nearly the same value. Attempts to alter any one set of a 's or $\Delta\nu$'s is found to alter other sets of a 's or $\Delta\nu$'s in such a way as to make conditions worse. Just how much, from the theoretical standpoint, a_1 ($4s$) should be changed by a change in the electron configuration, for example from $3d^5 4s 4p$ to $3d^6 4s$, is difficult to determine. The agreement between the a_1 's within each of the electron configurations is as good as can be expected.

The narrow hfs -separations in the 4D terms of Fig. 4 and the wide separations in the 6D terms show that the coupling of the six $3d$ electrons with the nucleus almost neutralizes that of the $4s$ electron. This same effect is also found in the b^6P^0 terms of Fig. 3. It should here be stated that preliminary calculations of a_1 , a_2 , and a_4 for the first nine terms of Table IV, omitting the l value of the $4p$ electron a_3 , indicated that the inclusion of the l value would give more constant values of a_1 and a_2 .

A study of Figs. 2, 3, and 4 and a comparison of these figures with Tables IV, V, and VI shows that only a few of the interesting relations to be found between the hfs and the gs of manganese have been pointed out above. This investigation has been carried on at Professor Paschen's laboratory at the Physikalisch-Technische Reichsanstalt, Berlin.